Modeling of Ethylbenzene Dehydrogenation Membrane Reactor to Investigate the Potential Application of a Microporous Hydroxy Sodalite Membrane

Mohammad Javad Vaezi[1,2], Ali Akbar Babaluo[1, 2*] and Sirous Shafiei[2]
[1]Nanostructure Material Research Center (NMRC), Sahand University of Technology, Tabriz, Iran
[2]Department of Chemical Engineering, Sahand University of Technology, Tabriz, Iran
(Received 18 February 2015, Accepted 22 March 2015)

Abstract

In this study the catalytic dehydrogenation of ethylbenzene to styrene was investigated in a simulated tubular sodalite membrane reactor. The high quality microporous sodalite membrane was synthesized by direct hydrothermal method and characterized by single gas permeation measurements. The performance of the prepared membrane showed high potential for application in a dehydrogenation membrane reactor (MR). The performance of the MR was evaluated using a pseudo-homogeneous model of the fixed bed that was developed in this purpose. The obtained results were evaluated in comparison with corresponding predictions for a plug flow reactor (PFR) operated at the same conditions. The modeling results confirmed the high performance of a MR over a conventional PFR. Ethylbenzene conversion and styrene yield increased about 3.45% and 8.99% respectively which is attributed to the effect of hydrogen removal from reaction side. The results demonstrate that the styrene yield in the MR is predicted to be more effective than that of in the conventional PFR.

Keywords: Ethylbenzene dehydrogenation, Membrane reactor, Microporous membrane, Simulation, Sodalite membrane

Introduction

Styrene as one of the most important monomers, is mainly produced via ethylbenzene dehydrogenation at operating temperatures of 823-923 K and atmospheric or sub-atmospheric pressure in the presence of commercial Fe_2O_3 catalyst [1-3]. One of the main problems in the actual ethylbenzene dehydrogenation process is the need for reactant recycle. This problem is due to the thermodynamic limitations and high endothermicity of the reaction resulting in the low conversion per pass [1]. So that, an attractive technique for breaking this limitation is the use of selective membranes in order to remove at least one of the products from the reaction media [4]. In this regard, membrane reactor is a type of multifunctional reactors and is currently being applied to many chemical reactions worldwide [5]. By the use of MR for dehydrogenation reactions, the reaction can be carried out at lower temperatures [3,6-7]. The lower operating temperature in a MR can be a suitable solution to the above mentioned problems, as hydrogen removal from the reaction side leads to enhancement of conversion and then styrene production [8]. The combination of catalysis and gas separation requires a membrane with high selectivity, adequate permeating rate, mechanical, thermal and chemical stability [4]. Considering the some drawbacks of palladium membrane as early membrane reactors studied for styrene dehydrogenation such as these membranes cost, permeability and stability, recently various studies focused on the enhancement of microporous zeolite membrane performance in dehydrogenation processes [3,9-10].

* Corresponding author: Tel: +984123458084 Email: a.babaluo@sut.ac.ir

Due to the high separation potential of zeolite membranes based on their molecular sieving and selective adsorption, this type of membranes are frequently applied in MR systems [3,6-7,10-14]. Among the zeolites, hydroxysodalite is crystalline aluminosilicate with a three dimensional channel network and pore size of 2.8 Å [15]. Because of the small pore size and high ion exchange capacity, sodalite has attracted considerable attentions [16]. So, this zeolite can be an ideal candidate for the separation of small molecules such as H_2 (2.89 Å) from gas mixtures [17].

As mentioned above, membrane reactor efficiency and its performance are highly associated to its membrane performance and one of the most important parameters that affects this efficiency is the performance of membrane at reaction conditions. Therefore, in this work, sodalite membrane was synthesized on the outer surface of homemade macroporous tubular ceramic support via hydrothermal method. Then, for the first time the performance of this kind of membrane was investigated at high temperatures. Also the empirical correlations for the permeation of gases through sodalite membrane as a function of temperature have been developed. Then, the simulation results which compare the performance of two types of reactor systems (a MR consisting of a sodalite on α-alumina support and a PFR) were investigated.

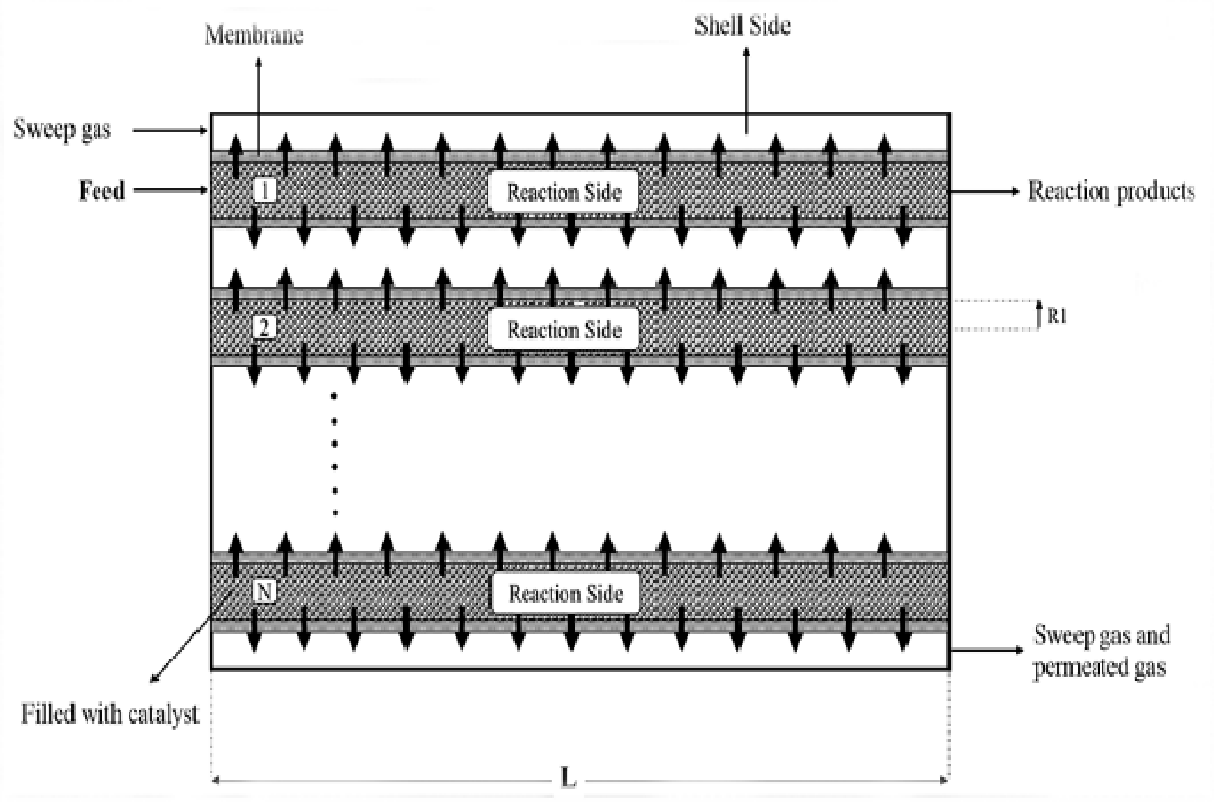

Figure 1: A schematic representation of the membrane reactor

2. Theory

2.1. Model Development

In order to evaluate the potential performance of hydroxysodalite membrane in the MR of ethylbenzene in comparison with a conventional PFR, a mathematical model was developed. The model is based on the governing equations describing a conventional PFR operation, taking into account the experimental permeation measurements correlated by an equation. The schematic representation of the membrane reactor is presented in Figure 1

2.2. Assumption

In order to derive the governing equations used to represent the MR operation, the following assumptions are adopted:

- Steady state operation
- Reaction occurs only inside the catalyst bed on the reaction (tube) side and the mixture of EB and nitrogen is fed into the reaction side at gas state
- Nitrogen as sweep gas is introduced to the shell side (permeate side) because using the steam at sodalite membrane reactor is not possible (the membrane would be blocked immediately)
- The sweep gas in shell side and feed in tube side are assumed to flow in co-current mode
- The effectiveness factors of reaction rates are taken to be equal to unity
- Temperatures of tube and shell side are the same
- Plug flow for both shell and tube sides is assumed
- Catalyst deactivation is neglected
- The pressure drop along the catalyst bed (tube side) is calculated based on Ergun's equation
- Pressure drop at permeate side is neglected

2.3. Reaction Kinetics

The reaction network for the dehydrogenation of EB to SM in the absence of steam is [2]:

$$C_6H_5CH_2CH_3 \Leftrightarrow C_6H_5CHCH_2 + H_2 \quad (1)$$

$\Delta H_{298\,K}$=117.6 kJ.mol^{-1}

$$C_6H_5CH_2CH_3 \rightarrow C_6H_6 + C_2H_4 \quad (2)$$

$\Delta H_{298\,K}$ = 105.4 kJ.mol^{-1}

$$C_6H_5CH_2CH_3 + H_2 \rightarrow C_6H_5CH_3 + CH_4 \quad (3)$$

$\Delta H_{298\,K}$ = -54.6 kJ.mol^{-1}

The corresponding rate equations, expressed as functions of component partial pressure in bars, are [2]:

$$r_1 = k_1 \times \left(P_{EB} - \frac{P_{SM} \times P_{H_2}}{K_P}\right) \quad (4)$$

$$r_2 = k_2 \times P_{EB} \quad (5)$$

$$r_3 = k_3 \times P_{EB} \times P_{H_2} \quad (6)$$

Where rate constants are defined as:

$$k_i = \exp\left(A_i - \frac{E_i}{RT}\right) \quad (7)$$

The numerical values of A_i and E_i are listed in Table1 [2]. With these constants, the reaction rates are expressed in kmol.kg cat^{-1}.h^{-1}.

Also Table 2 lists the enthalpy data used for the simulation [18].

Table 1: Arrhenius equation and equilibrium constants for ethylbenzene reactions (Abo-ghander et al., 2008)

Reaction No.	Enthalpy of Reaction: $\Delta H_R = a + bT + cT^2$		
	a[J.mol^{-1}]	b[J.mol^{-1}.K^{-1}]	c[J.mol^{-1}.K^{-2}]
1	115000	26.83	-0.01378
2	106700	-2.798	-0.002446
3	-46290	-28.89	0.009625

Table 2: Enthalpy correlation and its constants for ethylbenzene reaction network (Hermann et al., 1997)

Reaction No.	Frequency factor	Activation energy, kJ.mol^{-1}
1	0.85	**90.0**
2	14.00	**208.1**
3	0.56	**91.5**
Equilibrium constant K_A=exp(-ΔF/RT)		
$\Delta F = a + bT + cT^2$		
a= 122725.157 kJ.kmol^{-1}		
b = -126.2674 kJ.kmol^{-1}.K^{-1}		
c = -2.194×10^{-3}kJ.kmol^{-1}.K^{-2}		

2.4. Governing Equation for Membrane Reactor

To obtain the mole balance equations, a differential element along the axial direction inside the MR was considered. The processes occurring in the tube and shell side of MR are represented by mass balance equations as follows:

$$\frac{dF_{ti}}{dZ} = (1-\varphi)\pi R_1^2 \rho_{Catalyst} \sum_{j=1}^{3} (\pm\beta_{ij} r_j) \pm 2\pi R_1 J_i \Delta P \quad (8)$$

$$\frac{dF_{si}}{dZ} = \pm 2\pi N R_3 J_i \Delta P \quad (9)$$

In Eq. (8) "β_{ij}" is stoichiometric coefficient of reactant i in reaction j. In Eq. (9), "N" is the number of membrane tubes. The flux term "Ji" in Eqs. (8) and (9) is only applied to hydrogen; this term disappears for all other components. The hydrogen flux through the membrane is obtained by experimental data.

The energy balance for MR among the axial direction is obtained by:

$$F_T C_P \frac{dT}{dZ} = -\pi R_1^2 \rho_{Catalyst} \sum_{j=1}^{3} (\pm \Delta H_j r_j) \quad (10)$$

The pressure drop at the tube side is expressed as:

$$\frac{dP_{tT}}{dZ} = -150 \times 10^{-5} \frac{\mu_t u_{tz}}{(2r_p)^2} \frac{(1-\varphi_b)^2}{\varphi_b^3} - 1.75 \times 10^{-5} \frac{\rho_g u_{tz}^2}{2r_p} [\frac{1-\varphi_b}{\varphi_b^3}] \quad (11)$$

The mole fraction and partial pressure for tube and shell side are:

$$P_{ti} = \frac{F_{ti} \times P_{tT}}{\sum_{i=1}^{8} F_{ti}} \quad (12)$$

$$P_{si} = \frac{F_{si} \times P_{SM}}{\sum_{i=1}^{2} F_{si}} \quad (13)$$

$$y_{si} = \frac{F_{si}}{\sum_{i=1}^{2} F_{si}} \quad (14)$$

$$y_{ti} = \frac{F_{ti}}{\sum_{i=1}^{8} F_{ti}} \quad (15)$$

2.5. Numerical Solution

The final model consist of a system of 12 ordinary differential equations (ODEs) with the corresponding initial conditions was solved by the fourth order RungeKutta routine method.

2.6. Boundary Condition

For the co-current operation case, the set of equations give an initial value problem. So the boundary conditions are:

At Z = 0

Tube side: $F_{ti}=F_{ti0}$, (16)
$T=T_0$, $P_t=P_{t0}$
Shell side: $F_{si}=F_{si0}$, (17)
$T=T_0$, $P_s=P_{s0}$

2.7. Operating Condition

The operating conditions for both sides of the membrane reactor are given in Table 3. At the first step, the MR modeling results for only the main reaction of ethylbenzene dehydrogenation were compared with the confirmed modeling results of Gobina's work [19] and validated. Then the modeling procedure was expanded to the mentioned MR conditions and reactions.

3. Experimental

The tubular hydroxysodalite membrane used in this study was synthesized via direct hydrothermal method. The membrane had a multilayer asymmetric structure consist of an α-alumina tube (12 mm outer diameter, 3 mm inner diameter, 7 cm length, 570 nm mean pore diameter), and several outside hydroxysodalite layers. The synthesis solution was prepared by mixing the aluminate and silicalite solutions. The aluminate solution was prepared by dissolving sodium hydroxide (>99%, Merck) in deionized water followed by the addition of pure aluminum (>99%, Merck). The silicalite solution was made by mixing sodium hydroxide and deionized water with silica sol (>99%, Merck). The two solutions were mixed for 15 min in order to produce a homogenous solution. Synthesis was carried out at 363 K for 12 h, after which the tube was thoroughly washed with water until the pH of the residue was about neutral. Single gas permeation experiments were used to evaluate the separation performance of the membrane. It should be noted that the procedure of membrane synthesis was explained with more details in our previous work [20].

Table 3: Operating conditions for sodalite membrane reactor dehydrogenation reaction of ethylbenzene to styrene

Parameter	Value and dimensions
Inlet Temperature	853 K
Inner Diameter of Tube	16 mm
Outer Diameter of Tube	22 mm
Effective thickness of Membrane	20 μm
Catalyst Density	1500 $kg.m^{-3}$
Diameter of Catalyst Particle	2 mm
Void Fraction of Catalyst	0.6
Length of the reactor	1 m
Surface area of membrane	6900 m^2
Feed molar flow rates of Ethylbenzene at tube side	150 $mol.s^{-1}$
Feed molar flow rates of Nitrogen at tube side	220 $mol.s^{-1}$
Feed molar flow rates of Nitrogen at shell side	30 $mol.s^{-1}$

4. Result and Discussion

4.1. Membrane Characterization

Fig. 2 displays a result summary of the gas permeation experiments related to H_2, N_2 and CH_4 at 308 K. As can be seen, perm-selectivity of H_2 over N_2 and CH_4 is near to Knudsen mechanism. More investigation about the effect of temperature on the performance of the membrane showed that over 373 K the permeance of gases except H_2 is not measurable. So this result shows efficient H_2 separation performance of sodalite membrane for membrane reactor applications. Also, the results of gas permeation measurements of benzene, toluene, ethylbenzene and styrene monomer at temperatures higher than their boiling points show no permeation for them. Considering the kinetic diameters of the investigated gases, it can be claimed that the size of intercrystalline pores in the synthesized membrane cannot be higher than 5Å.

The gas permeation results presented in Fig. 3 clearly indicate the pressure independency of H_2 permeance. So the H_2 permeance at high temperatures can be correlated as function of temperature only:

$$Permeance = 1.925377061 \times 10^{22} \times T^{-12.22428129} \quad (18)$$

4.2. Modeling Result

Figs. 4 and 5 show the flow rate profiles of hydrogen and ethylbenzene evolved in a conventional PFR and MR respectively. In the conventional PFR and MR (Fig. 5), ethylbenzene flow rate decreases. But, hydrogen flow rate increases, passes through a maximum and then decreases again due to selective removal through the membrane (tube side) and also consumption in side reactions (Fig. 4). Also, hydrogen permeation rate is much lower than the hydrogen formation rate near the entrance of the reactor and thus the MR operates similar to a conventional PFR because the partial pressure of ethylbenzene and the rate of reaction are high, but the amount of produced hydrogen is low (low driving force for membrane diffusion). It can be concluded that by increasing of hydrogen partial pressure and thus its permeation rate, the MR becomes much more efficient than the PFR. Hydrogen removal from the reaction side (Fig. 4) shifts the equilibrium to the products side and increases the ethylbenzene conversion and decreases the flow rate of ethylbenzene both in PFR and MR.

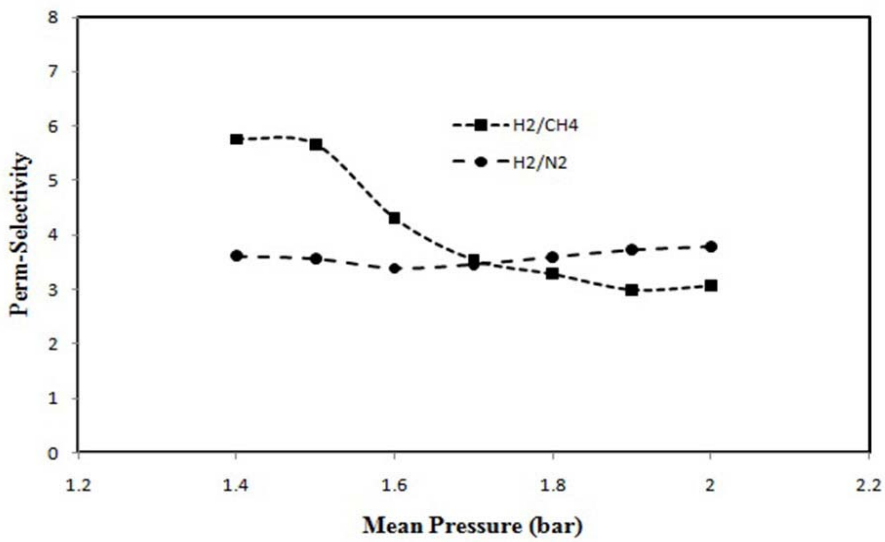

Figure 2: Perm-selectivity of H_2 over N_2 and CH_4 versus average pressure (bar) at 308 K

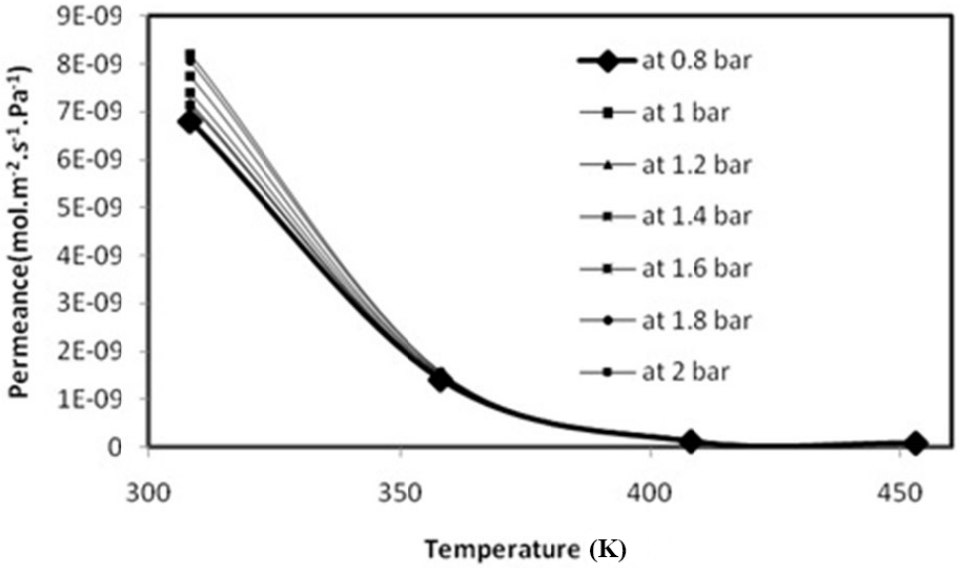

Figure 3: Permeance of H_2 versus temperature at different pressure through the membrane

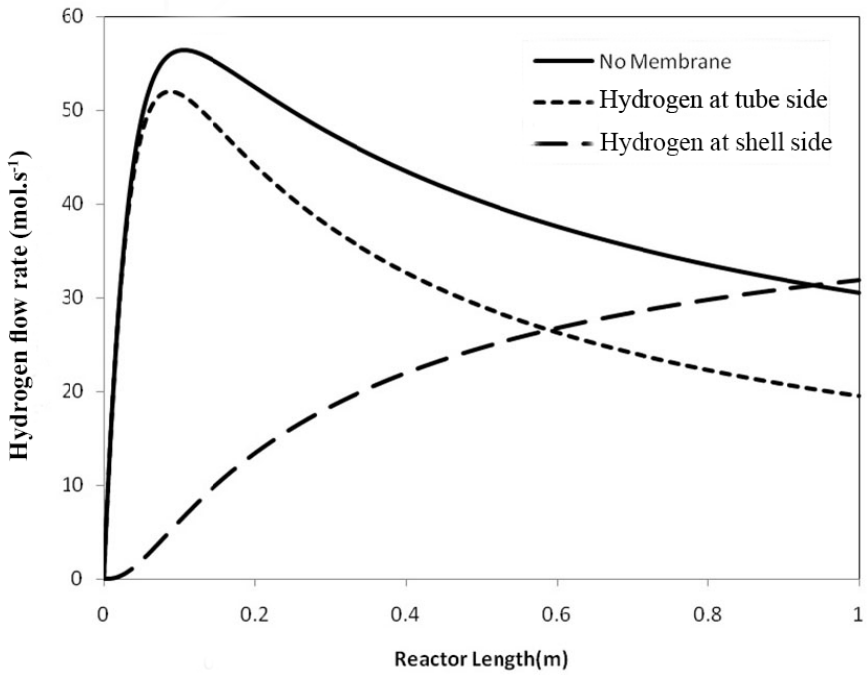

Figure 4: Molar flow of hydrogen on conventional PFR and the sodalite membrane reactor

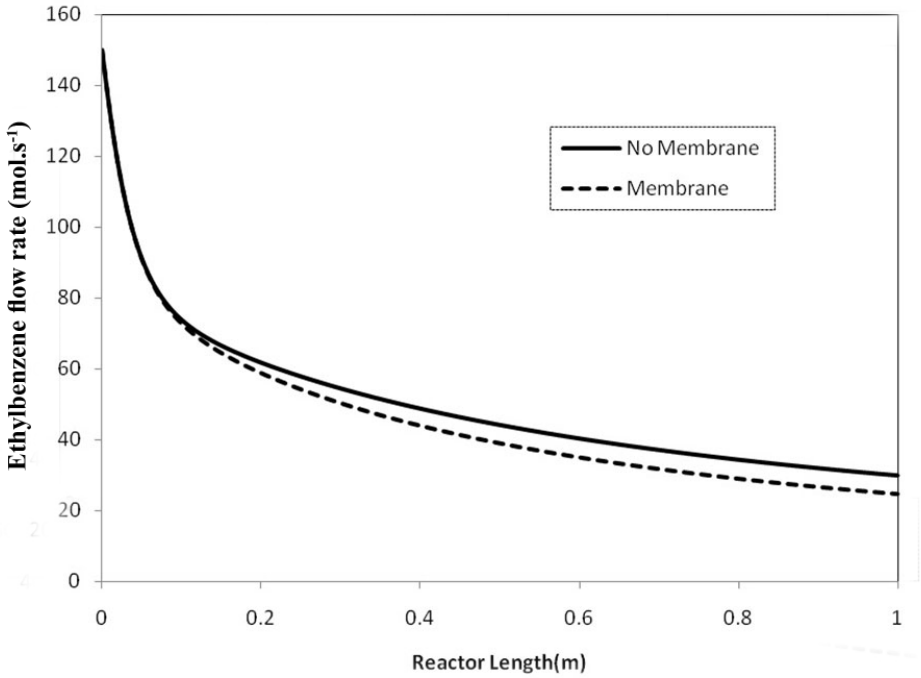

Figure 5: Molar flow of ethylbenzene on conventional PFR and the sodalite membrane reactor

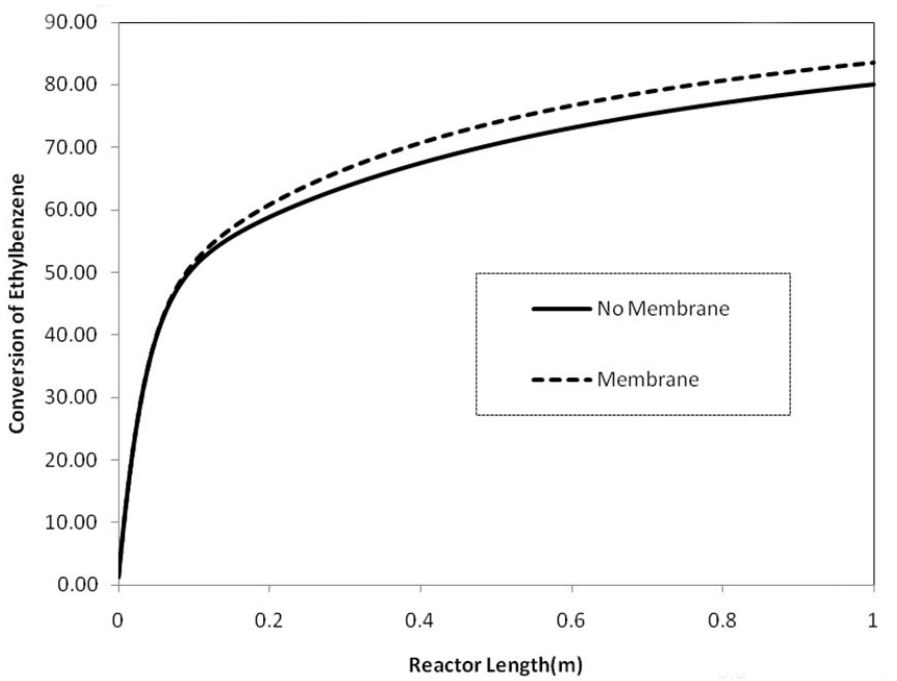

Figure 6: Comparison of ethylbenzene conversions between the conventional PFR and the sodalite membrane reactor

The ethylbenzene conversion and yield of styrene for sodalite membrane reactor and PFR are shown in Figs. 6 and 7. The maximum conversion and yield that can be attained in a conventional PFR at mentioned conditions are about 80% and 44.5% respectively due to thermodynamic limitations. In contrast, the maximum conversion and yield that can be attained in a MR with the characteristics described above, approach 83.45% and 53.49% respectively. So, using sodalite membrane reactor can increase ethylbenzene conversion and yield about 3.45% and 8.99% respectively. The membrane reduces the decreasing of ethylbenzene in MR (due to reduce the side reactions) and increase the yield of styrene in MR in comparison with PFR (Fig. 7).

Fig. 8 shows the temperature of MR and PFR as a function of reactor length. As expected, the temperature decreases with the length of reactors due to the high endothermic reaction of dehydrogenation of ethylbenzene to styrene. As can be seen, the temperature drop in MR is higher than PFR. This can be explained as membrane performance leads to increase in the conversion of dehydrogenation reaction and so decreases temperature more than PFR.

5. Conclusion

This study focused on the investigation of microporous sodalite membrane, for application of MR in ethylbenzene dehydrogenation. Single gas permeation experiments were used to evaluate the performance of the synthesized membrane. The experimental results revealed that the sodalite membrane has fair potential for dehydrogenation MR applications. A simple model was used to evaluate the MR performance for ethylbenzene dehydrogenation. The modeling results showed that the sodalite membrane reactor is more efficient than a conventional PFR. The magnitude of styrene yield increase which is achieved using sodalite membrane reactor, is appreciable.

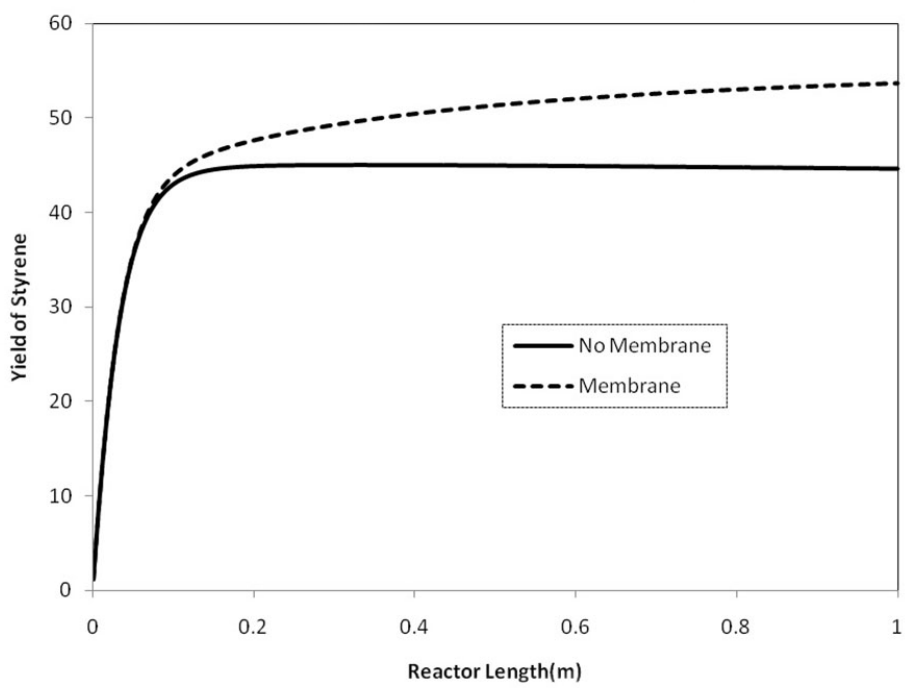

Figure 7: Comparison of styrene yields between the conventional PFR and the sodalite membrane reactor

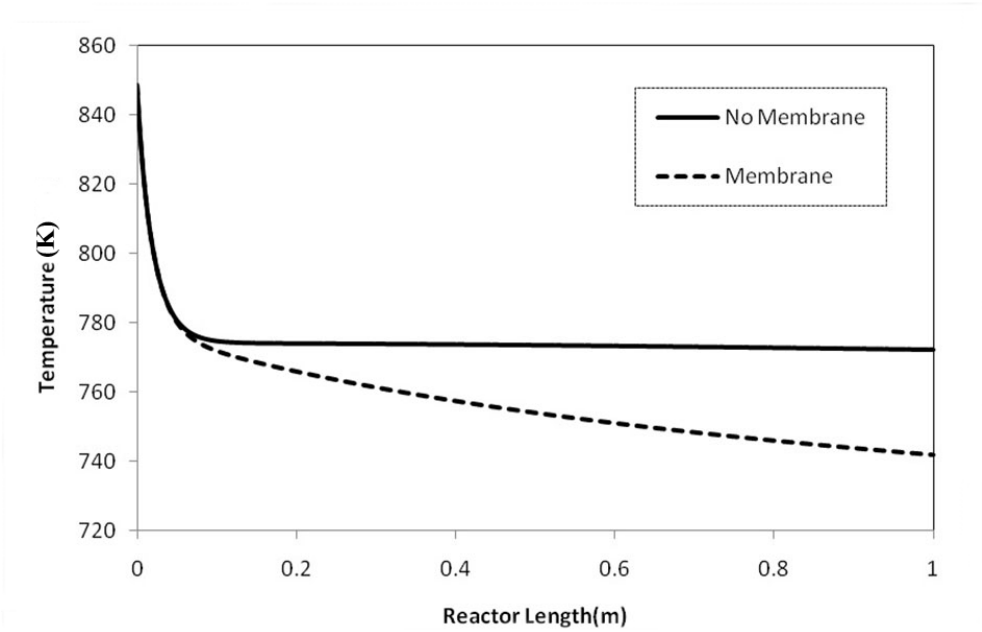

Figure 8: Comparison of temperature drop between the conventional PFR and the sodalite membrane reactor

Acknowledgment

The Authors wish to thank Sahand University of Technology (SUT) for the financial support of this work. Also, thank co-workers and technical staff in the chemical engineering department, Institute of nanostructure materials research center of SUT for their help during various stages of this work.

Notation

A_i	Frequency Factor, dimensionless
β_{ij}	Stoichiometric coefficient of reactant *i*in reaction *j,* dimensionless
C_p	Heat capacity of gaseous mixture in reactor, $J.mol^{-1}.K^{-1}$
E_i	Activation Energy, $kJ.mol^{-1}$
F_{ti}	Molar flow rate of component *i* at tube side, $mol.s^{-1}$
F_{si}	Molar flow rate of component *i* at shell side, $mol.s^{-1}$
F_{ti0}	Initial molar flow rate of component *i* at tube side, $mol.s^{-1}$
F_{si0}	Initial molar flow rate of component *i* at shell side, $mol.s^{-1}$
F_T	Total molar flow rate of gaseous mixture, $mol.s^{-1}$
J_i	Permeance of component *i* through membrane, $mol.m^{-2}.s^{-1}.bar^{-1}$
ΔH_j	Enthalpy of reaction, $J.mol^{-1}$
N	Number of membrane tube, dimensionless
P_{EB}	Partial pressure of ethylbenzene, bar
P_{SM}	Partial pressure of styrene, bar
P_{H2}	Partial pressure of hydrogen, bar
P_{si}	Partial pressure of reactant i at shell side, bar
P_{ti}	Partial pressure of reactant i at tube side, bar
P_{sT}	Total pressure at shell side, bar
P_{tT}	Total pressure at tube side, bar
P_{t0}	Initial pressure of tube side at Z=0, bar
P_{s0}	Initial pressure of shell side at Z=0, bar
ΔP	Pressure difference between shell and tube side, bar
r_i	Rate of reaction *i*, $mol.s^{-1}.kg\ of\ cat^{-1}$
r_P	Radius of catalyst particle, m
R	Gas constant = 8.314, $J.mol^{-1}.K^{-1}$

R_1	Inner diameter of tube, m
T_0	Initial inlet temperature, K
T	Temperature, K
k_i	Rate constant of reaction *i*, kmol.kg cat $^{-1}$.h $^{-1}$
K_P	Equilibrium constant of main reaction, bar
u_{tz}	Superficial velocity of gas in tube in z direction, m.s^{-1}
y_{si}	Mole fraction of component i in shell, dimensionless
y_{ti}	Mole fraction of component i in tube, dimensionless
Z	Axial direction, m

Greeks Symbol

φ	Porosity of catalyst, dimensionless
φ_b	Void fraction of packed catalyst bed in reaction side, dimensionless
$\rho_{catalyst}$	Density of catalyst, kg.m^{-3}
ρ_g	Density of gaseous mixture, kg.m^{-3}
μ_t	Viscosity of gaseous mixture in tube, bar.s

Abbreviation

EB	Ethylbenzene
SM	Styrene monomer

References:

1-Cavani, F. and Trifir, F.(1995). "Alternative processes for the production of styrene." *Appl. Catal*, A., Vol. 133, pp. 219-239.

2- Abo-ghander, N.S., Grace, J.R., Elnashaie, S.S.E.H. and Lim, C.J. (2008)."Modeling of a novel membrane reactor to integrate dehydrogenation of ethylbenzene to styrene with hydrogenation of nitrobenzene to aniline." *Chem. Eng. Sci*, Vol. 63, pp. 1817-1826.

3-Kong, C., Lu, J., Yang, J. and Wang, J. (2007)."Catalytic dehydrogenation of ethylbenzene to styrene in a zeolite silicalite-1 membrane reactor." *J. Membrane Sci*, Vol. 306, pp. 29-35.

4- Abdalla, B.K. and Elnashaie, S.S.E.H. (1993)."A membrane ethylbenzene reactor for the production of styrene from Ethylbenzene." *J. Membrane Sci*, Vol. 85, pp. 229-239.

5- Kumar, Sh., Shankar, S., Shah, P.R. and Kumar, S. (2006)."A Comprehensive Model for Catalytic Membrane Reactor." *Int. J. Chem. React. Eng*, Vol. 4, A5.

6- Bergh, J.V.D., Gücüyener, C., Gascon, J. and Kapteijn, F. (2011)."Isobutane dehydrogenation in a DD3R zeolite membrane reactor." *Chem. Eng. J*, Vol. 166, pp. 368-377.

7- Salomón, M.A., Coronas, J., Menéndez, M. and Santamar, J. (2000)."Synthesis of MTBE in zeolite membrane reactors." *Appl. Catal., A*, Vol. 200, pp. 201-210.

8-Koutsonikolas, D., Kaldis, S., Zaspalis, V.T. and Sakellaropoulos, G.P. (2012)."Potential application of a microporous silica membrane reactor for cyclohexane dehydrogenation." Int. *J. Hydrogen Energ*, Vol. 37, pp. 16302-16307.

9-She, Y., Han, J. and Ma, Y.H. (2001)."Palladium membrane reactor for the dehydrogenation of ethylbenzene to styrene." *Catal. Today*, Vol. 67, pp. 43-53.

10- Illgen, U., Schafer, R., Noack, M., Kolsch, P., Kuhnle, A. and Caro, J. (2001)."Membrane supported catalytic dehydrogenation of iso-butane using an MFI zeolite membrane reactor." *Catal. Commun*.,Vol. 2, pp. 339-345.

11- Jeong, B.H., Sotowa, K.I. and Kusakabe, K. (2003). "Catalytic dehydrogenation of cyclohexane in an FAU-type zeolite membrane reactor." J. *Membrane Sci*., Vol. 224, pp. 151-158.

12- Khajavi, Sh., Jansen, J.C. and Kapteijn, F. (2010a)."Application of a sodalite membrane reactor in esterification - Coupling reaction and separation." *Catal. Today*, Vol. 156, pp. 132-139.

13- Bernal, M.P., Coronas, J., Menendez, M. and Santamara, J. (2002)."Coupling of reaction and separation at the microscopic level: esteriÿcation processes in a H-ZSM-5 membrane reactor." *Chem. Eng. Sci*., Vol. 57, pp. 1557-1562.

14- Casanave, D., Fendler, A.G., Sanchez, J., Loutaty, R. and Dalmon, J.(1995). "Control of transport properties with a microporous membrane reactor to enhance yields in dehydrogenation reactions." *Catal. Today*, Vol. 25, pp. 309-314.

15- Naskar, M.K., Kundu, D. and Chatterjee, M.(2006). "Effect of process parameters on surfactant-based synthesis of hydroxy sodalite particles." Mater. Lett., Vol. 65, pp. 436-438.

16- Jiang, J., Gu, X., Feng, L., Duanmu, Ch., Jin, Y., Hu, T. and Wu, J. (2012)."Controllable synthesis of sodalite submicron crystals and microspheres from palygorskite clay using a two-step approach." *Powder Technol*., Vol. 217, pp. 298-303.

17- Khajavi, Sh., Sartipi, S., Gascon, J., Jansen, J.C. and Kapteijn, F. (2010)."Thermostability of hydroxy sodalite in view of membrane applications." *Micropor. Mesopor. Mat*, Vol. 132, pp. 510-517.

18- Hermann, Ch., Quicker, P. and Dittmeyer, R. (1997)."Mathematical simulation of catalytic dehydrogenation of ethylbenzene to styrene in a composite palladium membrane reactor." *J. Membrane Sci*., Vol. 136, pp. 161-172.

19- Gobina, E., Hou, K. and Hughes, R. (1995)."Mathematical analysis of ethylbenzene dehydrogenation: Comparison of microporous and dense membrane systems." J. Membrane *Sci.,* Vol. 105, pp. 163-176.

20- Kalantari, N., Vaezi, M.J., Yadollahi, M., Babaluo, A.A., Bayati, B. and Kazemzadeh, A. (2014). "Synthesis of nanostructure hydroxy sodalite composite membranes via hydrothermal method: support surface modification and synthesis method effects." *Asia Pac. J. Chem. Eng*., DOI: 10.1002/apj.1844.